ACS Catalysis

Letter

pubs.acs.org/acscatalysis

External Surface Catalytic Sites of Surfactant-Tailored Nanomorphic Zeolites for Benzene Isopropylation to Cumene

Wookdong Kim,[†,‡] Jeong-Chul Kim,[†,§] Jeongnam Kim,[‡] Yongbeom Seo,[†,‡] and Ryong Ryoo*[,†,‡]

[†]Center for Nanomaterials and Chemical Reactions, Institute for Basic Science, Daejeon 305-701, Korea

[‡]Department of Chemistry, KAIST, Daejeon 305-701, Korea

[§]Graduate School of Nanoscience and Technology (WCU), KAIST, Daejeon 305-701, Korea

Supporting Information

ABSTRACT: Nanomorphic *BEA, MTW, and *MRE zeolites were investigated as catalysts for isopropylation of benzene. From the deactivation pattern of the zeolites, we evaluated the contribution of external and internal active sites. These nanomorphic zeolites exhibited a high activity and long catalytic lifetime. Such catalytic properties can be explained by a large contribution of external sites, which have the advantage of slow deactivation.

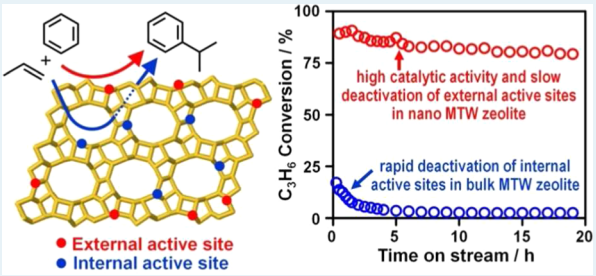

KEYWORDS: *zeolites, alkylation, heterogeneous catalysis, nanomorphic, external surface*

Zeolites are a family of crystalline microporous aluminosilicate materials, which are widely used as catalysts in petrochemical processing and various organic reactions.[1−3] Zeolites for catalytic applications are usually synthesized in the form of micrometer-sized crystallites. Despite such a small crystal size, the external surface of zeolite particles is still negligible in comparison with the enormous surface area of the internal micropore walls (<1 nm). Accordingly, chemical reactions occurring at the external surface are usually insignificant in comparison with the main reactions occurring inside micropores. In this situation, the molecular sieving effect of the micropores imparts to zeolites their well-known shape-selectivity in catalysis.[4,5] A typical example is the conversion of *m*-xylene to *p*-xylene over MFI zeolite (type material: ZSM-5).[6] For shape-selective catalytic applications, larger zeolite crystals have the advantage of higher selectivity than smaller crystals owing to a lesser portion of nonselective chemical reactions taking place at the external surface sites.[7,8]

Alkylations of benzene into ethylbenzene and *i*-propylbenzene (commonly known as cumene) are of high industrial importance and can be carried out using zeolite as an acid catalyst.[9−11] In particular, cumene synthesis can be performed by the alkylation of benzene with propene. Zeolites with *BEA and MTW structures (type materials: beta and ZSM-12, respectively) are known as efficient catalysts in the cumene synthesis process.[12,13] These zeolites have microporous channel structures composed of 12-membered oxygen rings (12-MR). BEA zeolite has a 3-dimensionally (3D) intersecting channel structure composed of two perpendicular straight channels with a cross section of 0.64 × 0.76 nm and a sinusoidal channel with a cross section of 0.55 × 0.55 nm. MTW zeolite has a 1D straight channel structure with a cross section of 0.57 × 0.61 nm. As in many other zeolite catalysis processes, the cumene synthesis reaction was thought to occur mainly inside these zeolite channels.[14] However, contrary to this common view, external surfaces were reported as highly active for the cumene synthesis reaction in a previous study of MWW structure zeolite (type material: MCM-22).[15] The catalytic activity of the zeolite external surfaces was attributed to the particular structure of half cavities or chalices. We show in this paper that the high catalytic performance of external surfaces can be generalized to other zeolites, such as MTW, *BEA, and *MRE (type material: ZSM-48). The benzene−propene reaction can take place predominantly on the external surfaces of these zeolites rather than on the internal micropore walls if the zeolites are synthesized in nanocrystals less than 10 nm in thickness. Furthermore, the reaction on the nanocrystal surfaces has the advantage of high catalytic activity and very long lifetime, as compared with conventional micrometer-sized crystals.

We synthesized nanocrystalline *BEA and MTW as well as *MRE zeolite via a surfactant-tailored synthesis route similar to the synthesis of MFI zeolite nanosheets.[16] Zeolite with *MRE structure had another type of 1D channels, but the pore channels were composed of a 10-MR cross section (0.53 × 0.56 nm). These zeolites were obtained as irregular 3D networks of nanocrystals (i.e., nanosponge or an assembly of nanosheets). The zeolite samples are designated as nanomorphic in this paper. In such nanomorphic zeolites, our catalytic investigation indicates that a large portion of the acid-catalyzed cumene

Received: October 18, 2012
Revised: January 3, 2013
Published: January 8, 2013

synthesis reactions can take place at acid sites located on the external surfaces. The external catalytic sites are much more slowly deactivated than the internal sites, probably because these sites are widely open to the gas phase and are accordingly unaffected by micropore blockage.[17] As a result, nanomorphic zeolites can exhibit high catalytic activity with a very long catalytic lifetime as compared with micrometer-sized ordinary zeolite samples (designated as bulk zeolites). This can be a remarkable advantage in many other acid-catalyzed chemical reactions, whereas deactivated zeolite catalysts need frequent regeneration or replacement. Among these nanomorphic zeolites, the nanomorphic MTW zeolite with extremely short 1D channels (<10 nm in length) exhibits the highest catalytic conversion and the longest catalytic lifetime.

The surfactant used for synthesis of the nanomorphic zeolites was $[C_{22}H_{45}-N^+(CH_3)_2-C_6H_{12}-N^+(CH_3)_2-CH_2-(C_6H_4)-CH_2-N^+(CH_3)_2-C_6H_{12}-N^+(CH_3)_2-CH_2-(C_6H_4)-CH_2-N^+(CH_3)_2-C_6H_{12}-N^+(CH_3)_2-C_{22}H_{45}](Br^-)_2(Cl^-)_4$. This hexaammonium surfactant is a hierarchical structure-directing agent (SDA) in which the zeolite SD modules are inserted between two C22-alkyl tails. In principle, the SD modules generate the micropores in the zeolite framework while the surfactant tails direct the zeolite crystal to grow in a nanomorphic manner. The nanomorphic *BEA was hydrothermally synthesized in an autoclave at 413 K as described elsewhere.[18] The MTW and *MRE zeolites were also obtained using the same surfactant. However, the methods of their synthesis were discovered for the first time in the present work. All the nanomorphic zeolite samples are designated by prefixing nano to the zeolite structure codes (e.g., nano-BEA) without the indication of polytypic structures by an asterisk. For comparison, the corresponding conventional zeolites were synthesized on the basis of the synthesis procedures reported in the literature.[19−21] The conventional zeolite samples are designated by prefixing bulk to the zeolite structure codes. Details of the synthetic procedures for the nanomorphic and bulk zeolites are given in the Supporting Information (SI). The zeolite structures were confirmed by high-resolution transmission electron microscopy (TEM) and X-ray powder diffraction (XRD).

All the synthesized zeolites exhibited XRD peaks corresponding to the *BEA, MTW, and *MRE structures (Figure 1a−c). The nanomorphic zeolites exhibited broad peaks as compared with their bulk counterparts. The line-broadening was consistent with the nanometer-sized zeolite crystals, which were assembled in an irregular manner to possess the intercrystalline mesopores. The nanocrystals were <10 nm in thickness (see the TEM images in Figure 1d−f). In particular, nano-MRE showed a much weaker (200) reflection than (015) and (033), as compared with its bulk counterpart. The low (200) diffraction intensity indicated that nano-MRE could have a nanosheet-like morphology, which was very thin along the *a*-axis of the MRE crystal structure. In good agreement with the structural information obtained from XRD and TEM, all the nanomorphic zeolite samples exhibited highly mesoporous textural properties in addition to the intrinsic microporosity of the zeolite. The nanomorphic zeolites exhibited high specific total surface areas as compared with their bulk counterparts (see Table 1). The porous textual properties were evaluated from the N_2 adsorption−desorption isotherms measured at 77 K (Figure S1 in the SI). The total specific surface area was determined by the Brunauer−Emmett−Teller (BET) method. Furthermore, each pair of nanomorphic and bulk zeolites was

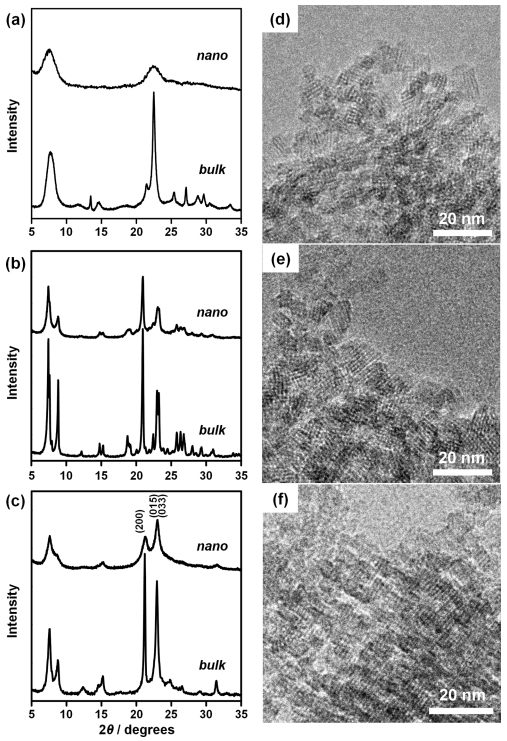

Figure 1. Powder XRD patterns of (a) nano-BEA, (b) nano-MTW zeolite, and (c) nano-MRE zeolite. TEM images of (d) nano-BEA, (e) nano-MTW zeolites, and (f) nano-MRE zeolite. For comparison, XRD patterns of their bulk counterparts are also provided.

Table 1. Physicochemical Properties of the Bulk and Nanomorphic Zeolites

zeolites	Si/Al	S_{BET}[a] ($m^2\ g^{-1}$)	V_{total}[b] ($cm^3\ g^{-1}$)	BA_{int}[c] ($\mu mol\ g^{-1}$)	BA_{ext}[d] ($\mu mol\ g^{-1}$)
bulk-BEA	11	490	0.24	1090	55
nano-BEA	13	820	1.49	604	306
bulk-MTW	45	280	0.14	258	8
nano-MTW	55	470	0.86	165	58
bulk-MRE	100	160	0.11	112	9
nano-MRE	110	380	0.47	86	26

[a] S_{BET} is the surface area calculated from the adsorption data using P/P_0 between 0.1 and 0.3 using the BET equation. [b] V_{total} is total pore volume obtained at $P/P_0 = 0.95$. [c] BA_{int} is the concentration of internal Brönsted acid sites, which was calculated by subtracting the concentration of external acid sites from that of total acid sites. [d] BA_{ext} is the concentration of external Brönsted acid sites.

synthesized to have very similar Si/Al ratios (Table 1) to minimize the effect of the Si/Al ratio on the catalytic properties. The Si/Al ratios were measured by elemental analysis using inductively coupled plasma atomic emission spectroscopy. The concentration of Brönsted acid sites was analyzed by a titration method using phosphine oxides as titrants, in which the acid strength can be detected by chemical shifts in the solid-state ^{31}P NMR spectroscopic signals of the phosphine oxides (see the Experimental section and Figure S3 in the SI).[22,23] Trimethylphosphine oxide was used as a titrant for the determination of "total acid sites", which means all acid sites that are located on internal pore walls and external surfaces. Tributylphosphine oxide was used as a selective titrant for external sites because its molecular diameter is greater than micropore apertures. The acid concentrations determined in

dx.doi.org/10.1021/cs300678n | ACS Catal. 2013, 3, 192−195

this manner are summarized in Table 1. These results show that the external acid sites are quite significant in the case of nanomorphic zeolites.

The benzene−propene reaction was carried out in a fixed-bed Pyrex reactor (10 mm inside diameter). A mixture of benzene and propene was fed into the catalyst bed, which was heated to 513 K (benzene/propene = 3 in molar ratio, WHSV of benzene = 8.8 h^{-1}). The products were analyzed as a function of time on stream (TOS) (see the Experimental section in the SI). The product distribution was investigated at 1 h of TOS. Each zeolite had cumene selectivity of more than 70% (see Table S1 in the SI). In Figure 2, the propene

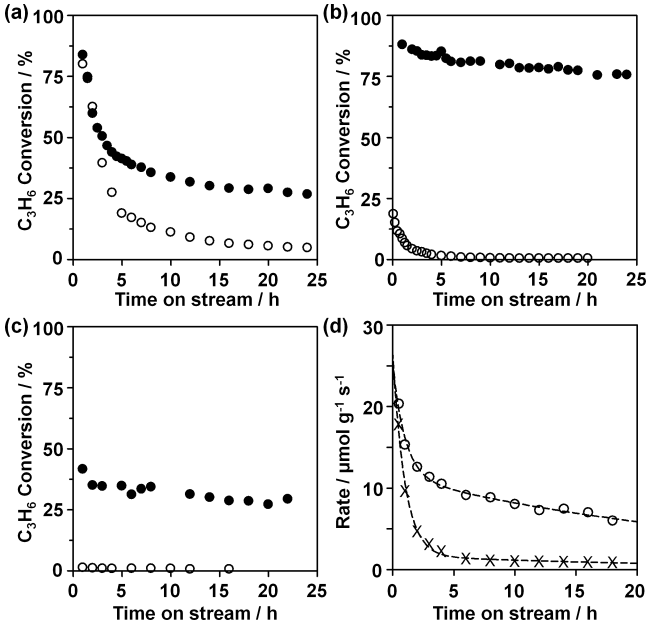

Figure 2. Propene conversion over (a) *BEA, (b) MTW, and (c) *MRE zeolites plotted as a function of time on stream (reaction conditions: WHSV of benzene = 8.8 h^{-1}, reaction temperature = 513 K). The nanozeolites (solid circles) showed higher conversion than bulk zeolites (open circles). (d) Reaction rate over nano-BEA (empty circles) and bulk-BEA (crosses) plotted as a function of time on stream (reaction conditions: WHSV of benzene = 88 h^{-1}, reaction temperature = 483 K). The dashed curves are the fits according to eq 2.

conversion is plotted against TOS. As the result shows, the bulk-MRE zeolite exhibited almost no conversion of propene, reflecting that the 10-MR pore apertures in the zeolite were not sufficiently wide for cumene diffusion. On the other hand, nano-MRE exhibited 42% conversion. The conversion difference between nano- and bulk-MRE indicates that the much higher catalytic activity of the nanomorphic zeolite is due to the external catalytic sites on the zeolite nanocrystals. In the cases of MTW and *BEA, the catalytic activity of the nanomorphic zeolites was also higher than that of their bulk counterparts, indicating the contribution of the external catalytic sites. However, the difference between nano and bulk was much less than that in the case of *MRE zeolite. It is reasonable to conclude that, in these 12-MR zeolites, the bulk zeolites could readily catalyze the cumene synthesis reaction inside micropores owing to the molecular diffusion through the 12-MR apertures.

In Figure 2, the bulk-BEA zeolite shows a steeply decreasing catalytic activity against TOS, and nano-BEA is deactivated slowly. In the case of MTW, the difference between nano and bulk is much more pronounced than that in the case of *BEA zeolites. The bulk-MTW catalyst initially exhibited 18% propene conversion and lost more than half the catalytic activity in 2 h. On the other hand, nano-MTW initially exhibited 88% conversion of propene, which was 4.4 times the initial propene conversion attained with bulk-MTW. Furthermore, the nano-MTW catalyst was able to maintain more than 60% of its initial catalytic conversion, even after 60 h. These deactivation phenomena can be analyzed according to the catalytic deactivation kinetics, assuming that the catalytic deactivation rate is proportional to the catalytic activity of a system consisting of identical active sites.[24,25] The kinetic analysis can be simplified by limiting the catalytic conversion to such a sufficiently low value (e.g., <20% of the limiting reagent) that the reactant concentrations can be assumed as constant throughout a catalyst bed. Under this condition, the reaction rate becomes proportional to the catalytic conversion. Then the reaction rate becomes an exponentially decreasing function of TOS as follows:

$$r \propto e^{-kt} \tag{1}$$

where r is the reaction rate, t is the TOS, and k is the deactivation rate constant. In a zeolite, there are many catalytic sites with various acid strengths at different locations. We try to categorize them into "external surfaces" and "internal pores" according to their locations. In this case, eq 1 becomes

$$r = C_{int}e^{-k_{int}t} + C_{ext}e^{-k_{ext}t} \tag{2}$$

where C indicates the contribution factor to the total reaction rate. The subscripts "int" and "ext" refer to the internal and external sites, respectively. Equation 2 means that the total deactivation pattern can be expressed as a linear combination of internal and external reactions.

Figure 2d shows the experimental data fits for nano-BEA and bulk-BEA using eq 2. The experimental result was obtained with a high rate of reactant feeding (WHSV of benzene = 88 h^{-1}) at a low reaction temperature (483 K) so that the initial conversion of propene could be lower than 20%. The fitting parameters—C_{int}, k_{int}, C_{ext}, and k_{ext}—for the nano- and bulk-BEA zeolites are summarized in Table 2. The fitting result

Table 2. Summary of Fitting Parameters for Linear Combination of Deactivation Functions

zeolites	C_{int} [a] (μmol g^{-1} s^{-1})	k_{int} [b] (s^{-1})	C_{ext} (μmol g^{-1} s^{-1})	k_{ext} (s^{-1})
bulk-BEA	25.3	1.02	1.9	0.04
nano-BEA	13.7	0.97	11.4	0.04

[a] C is a contribution of each deactivation functions. [b] k is a deactivation rate constant.

shows that C_{int} was more than 10 times larger than C_{ext} in the case of the bulk-BEA catalyst. This means that the internal catalytic reaction dominated over the external surface reaction in the bulk zeolite. In the case of the nano-BEA catalyst, however, the external reaction became important (C_{ext}/C_{int} = 0.9). The C_{ext} value for nano-BEA was 6.0 times as much as C_{ext} for bulk-BEA. This ratio shows remarkable agreement with 5.6, which is the ratio of external acid concentrations between nano-BEA and bulk-BEA (obtained from the titration analysis using phosphine oxides). This agreement indicates that the high value of C_{ext} in the nanomorphic *BEA zeolite could be due to the

dx.doi.org/10.1021/cs300678n | ACS Catal. 2013, 3, 192−195

large contribution of catalytic reaction occurring at external acid sites. Moreover, the result of $k_{ext} \ll k_{int}$ indicates that the external catalytic sites were much more slowly deactivated than the internal sites. Thus, a large contribution of the external reaction could lead to a high initial catalytic activity and a very long catalytic lifetime in nanomorphic zeolite.

Among the investigated zeolites, the nano-MTW exhibited the highest contribution of the external reaction and, consequently, the highest propene conversion at 24 h of TOS. In this regard, the nano-MTW zeolite was much better as a cumene-synthesis catalyst than either the nano-BEA or bulk-BEA zeolite, at least under our reaction conditions. *BEA zeolites are often referred to as practical catalysts for industrial cumene synthesis.[26] Hence, the present nanomorphic form of MTW zeolite may be considered as a potential catalyst for cumene synthesis with high activity and long catalytic lifetime.

In summary, we investigated the catalytic alkylation of benzene with propene over nanomorphic *BEA, MTW, and *MRE zeolites in comparison with their bulk counterparts. All the nanomorphic zeolites exhibited remarkably higher conversion of propene and longer catalytic lifetime than ordinary crystalline zeolites. The catalytic performance could be explained by a linear combination of external surface reaction and internal pore reaction. The external contribution was insignificant in ordinary micrometer-sized crystalline zeolites, but in the nanomorphic zeolites, the external contribution was more important. Furthermore, the external catalytic sites in the nanomorphic zeolites had the advantage of slow deactivation. We confirmed that the nanomorphic zeolites also have the same type of advantage in the case of benzene ethylation with ethylene. We believe that this catalytic advantage could be extended to other zeolites with various structures and other catalytic reactions.

■ ASSOCIATED CONTENT

Supporting Information

Detailed experimental procedures for zeolite synthesis, characterization, and catalytic reaction; nitrogen adsorption−desorption isotherms, SEM images, ^{31}P NMR spectra, and reaction product distributions. This material is available free of charge via the Internet at http://pubs.acs.org.

■ AUTHOR INFORMATION

Corresponding Author

*E-mail: rryoo@kaist.ac.kr.

Notes

The authors declare no competing financial interest.

■ ACKNOWLEDGMENTS

This work was supported by the Research Center Program (CA1201) of IBS (Institute for Basic Science) in Korea.

■ REFERENCES

(1) Corma, A. *J. Catal.* **2003**, *216*, 298−312.
(2) Marcilly, C. *J. Catal.* **2003**, *216*, 47−62.
(3) Vermeiren, W.; Gilson, J.-P. *Top. Catal.* **2009**, *52*, 1131−1161.
(4) Csicsery, S. M. *Zeolites* **1984**, *4*, 202−213.
(5) Degnan, T. *J. Catal.* **2003**, *216*, 32−46.
(6) Kim, J.; Kunieda, T.; Niwa, M. *J. Catal.* **1998**, *439*, 433−439.
(7) Kaeding, W. W.; Chu, C.; Young, L. B.; Weinstein, B.; Butter, S. A. *J. Catal.* **1981**, *67*, 159−174.
(8) Fraenkel, D. *Ind. Eng. Chem. Res.* **1990**, *29*, 1814−1821.
(9) Kaeding, W. W.; Holland, R. E. *J. Catal.* **1988**, *109*, 212−216.
(10) Degnan, T. F., Jr.; Smith, C. M.; Venkat, C. R. *Appl. Catal., A* **2001**, *221*, 283−294.
(11) Han, M.; Lin, S.; Roduner, E. *Appl. Catal., A* **2003**, *243*, 175−184.
(12) Reddy, K. S. N.; Rao, B. S.; Shiralkar, V. P. *Appl. Catal., A* **1993**, *95*, 53−63.
(13) Pradhan, A. R.; Rao, B. S.; Shiralkar, V. P. In *Catalysis and Adsorption by Zeolites*; Ohlmann, G., Pfeifer, H., Fricke, R., Eds.; Elsevier Science Publishers B. V.: Amsterdam, 1991; Vol. *65*, p 347.
(14) Perego, C.; Amarilli, S.; Millini, R.; Bellussi, G.; Girotti, G.; Terzoni, G. *Microporous Mater.* **1996**, *6*, 395−404.
(15) Corma, A.; Martínez-Soria, V.; Schnoeveld, E. *J. Catal.* **2000**, *192*, 163−173.
(16) Choi, M.; Na, K.; Kim, J.; Sakamoto, Y.; Terasaki, O.; Ryoo, R. *Nature* **2009**, *461*, 246.
(17) Hughes, R. *Deactivation of Catalysts*; Academic Press: London, 1984; p 43.
(18) Na, K.; Jo, C.; Kim, J.; Cho, K.; Jung, J.; Seo, Y.; Messinger, R. J.; Chmelka, B. F.; Ryoo, R. *Science* **2011**, *333*, 328−332.
(19) Camblor, M. A.; Pérez-Pariente, J. *Zeolites* **1991**, *11*, 202−210.
(20) Ernst, S.; Jacobs, P. A.; Martens, J. A.; Weitkamp, J. *Zeolites* **1987**, *7*, 458−462.
(21) Lai, W. F.; Roth, W. J.; Kay, R. E.; Elia, C. N. (ExxonMobil) US Patent 8003074, 2011.
(22) Rakiewicz, E. F.; Peters, A. W.; Wormsbecher, R. F.; Sutovich, K. J.; Mueller, K. T. *J. Phys. Chem. B* **1998**, *102*, 2890−2896.
(23) Zhao, Q.; Chen, W.-H.; Huang, S.-J.; Wu, Y.-C.; Lee, H.-K.; Liu, S.-B. *J. Phys. Chem. B* **2002**, *106*, 4462−4469.
(24) Hughes, R. *Deactivation of Catalysts*, Academic Press: London, 1984; p 110.
(25) Chen, W.; Tsai, T.; Jong, S.; Zhao, Q.; Tsai, C.; Wang, I.; Lee, H.; Liu, S. *J. Mol. Catal. A: Chem.* **2002**, *181*, 41−55.
(26) Perego, C.; Ingallina, P. *Catal. Today* **2002**, *73*, 3−22.